Spin waves in quasi-periodic Fe/Cr(100) thin films

2002 J. Phys.: Condens. Matter 14 1785

(http://iopscience.iop.org/0953-8984/14/8/308)

INSTITUTE OF PHYSICS PUBLISHING JOURNAL OF PHYSICS: CONDENSED MATTER

J. Phys.: Condens. Matter **14** (2002) 1785–1797 PII: S0953-8984(02)26846-0

Spin waves in quasi-periodic Fe/Cr(100) thin films

P W Mauriz[1,2], E L Albuquerque[3,5] and C G Bezerra[3,4]

[1] Departamento de Física, Universidade Federal do Ceará, 60451-970, Fortaleza-CE, Brazil
[2] Departamento de Ciências Exatas, Centro Federal de Educação Tecnológica do Maranhão, 65025-001, São Luís-MA, Brazil
[3] Departamento de Física, Universidade Federal do Rio Grande do Norte, 59072-970, Natal-RN, Brazil
[4] Department of Physics and Astronomy, University of Western Ontario, London, Ontario, Canada N6A 3K7

E-mail: eudenilson@dfte.ufrn.br

Received 6 July 2001, in final form 4 January 2002
Published 15 February 2002
Online at stacks.iop.org/JPhysCM/14/1785

Abstract

In this work we have calculated the ferromagnetic (FM) resonance curves of Fe/Cr(100) thin films, which follow the Fibonacci sequence. Our approach is based on the equations of motion for the small-signal magnetization deviation from the equilibrium directions. The equilibrium positions of the magnetizations are calculated from the total energy, which includes the following contributions: *Zeeman*, *bilinear exchange*, *biquadratic exchange*, *dipolar*, *cubic anisotropy* and *surface anisotropy* terms. We also consider the presence of an external magnetic field applied in the plane of the films and parallel to the easy axes. The experimental parameters used in our calculations were recently reported and lie in three regions of interest, namely (i) near to the first antiferromagnetic (AF) peak (strong bilinear exchange coupling), (ii) near to the first FM–AF transition (moderate bilinear exchange coupling) and (iii) near to the second AF peak (weak bilinear exchange coupling comparable to the biquadratic exchange coupling). Our results show the effect of the quasi-periodic arrangement in the spin wave *dispersion relation* of these artificial structures.

(Some figures in this article are in colour only in the electronic version)

1. Introduction

Quasicrystals were discovered by Shechtman and co-workers [1] in 1984. They mixed aluminum and manganese in a roughly six-to-one proportion and heated the mixture until it melted. The mixture was then rapidly cooled back into the solid state by dropping the liquid

[5] Author to whom any correspondence should be addressed.

onto a cold spinning wheel, a process known as melt spinning. When the solidified alloy was examined, using an electron microscope, a novel structure was revealed. It exhibited fivefold symmetry, which is forbidden in crystals, and long-range order, which is lacking in amorphous solids. Its order, therefore, was neither amorphous nor crystalline.

Levine and Steinhardt [2] introduced the term quasicrystal for this special incommensurate structure. The origin of the name quasicrystal, also called *quasi-periodic crystal* (for a review see [3–5]), arises from the fact that these materials have quasi-periodic translational order, as opposed to the periodic order of ordinary crystals. It can be examined in terms of a high-resolution electron micrograph. The rows of bright spots are separated by small and large intervals. As in the Penrose pattern [6], the length of the large interval divided by the length of the small one is equal to the *golden mean* number, $\tau = \frac{1}{2}(1 + \sqrt{5})$, and the sequence of large and small intervals reproduces the Fibonacci sequence. Moreover, they suggested that the translational order of atoms in quasi-crystalline alloys might be quasi-periodic rather than periodic.

The procedure to grow quasi-periodic superlattices became standard after the work of Merlin *et al* [7], who reported the realization of the first quasi-periodic superlattice, consisting of alternating layers of GaAs (building block A) and AlAs (building block B), following the Fibonacci sequence by means of molecular beam epitaxy (MBE). Since then, the behaviour of a variety of particles or quasi-particles (electrons, phonons, photons, polaritons, magnons etc) has been and is currently being studied in quasi-periodic systems [8–10].

A quite interesting characteristic of these quasi-periodic crystals is the fact that they display collective properties, due to the presence of long-range correlations, that are not shared by their constituents. Besides, apart from their theoretical relevance, they have potential technological interest in several areas.

In a quasi-periodic system, all the states are critical. The wavefunctions are neither Bloch-type extended states, as in periodic systems, nor exponentially localized states, as in disordered systems. The wave spectrum has a singular continuous character, so they can be defined as systems intermediate between periodic crystals and random amorphous solids, defining a novel description of disorder [11]. The energy spectrum also has a rich self-similar structure, with various scaling indices. The gaps are distributed densely and there are no isolated states. Thus they define a Cantor set, with zero Lebesgue measure [12]. The profile of the integrated density of states resembles very much the shape of the devil's staircase. When the quasiperiodicity is stronger, the spectra are more fractured, with a multiplicity of gaps [13].

Parallel to these developments in the field of quasicrystals, the properties of magnetic exchange interactions between FM films separated by nonmagnetic spacers have also been widely investigated [14]. The discovery of physical properties such as AF exchange coupling [15], giant magnetoresistance (GMR) [16], oscillatory behaviour of the exchange coupling [17] and biquadratic exchange coupling [18] made these films excellent options for technological applications and attractive objects of research.

The spin wave dispersion relations for trilayer structures have been calculated by several authors. Solutions including, besides the usual exchange and dipolar contributions, the bilinear exchange coupling were worked out by Hillebrands [19], for an arbitrary number of magnetic layers. For a trilayer structure, formed by two magnetic films separated by a nonmagnetic spacer, the dispersion relation was obtained from a system of 16 linear equations. Rezende *et al* [20] presented model calculations for the trilayer structure, where the coupling between the magnetic fields through magnetic dipolar, bilinear and biquadratic exchange interactions was fully taken into account, together with surface, in-plane uniaxial and cubic anisotropies. Their approach was based on the equation of motion for the small-signal magnetization deviations from the equilibrium directions.

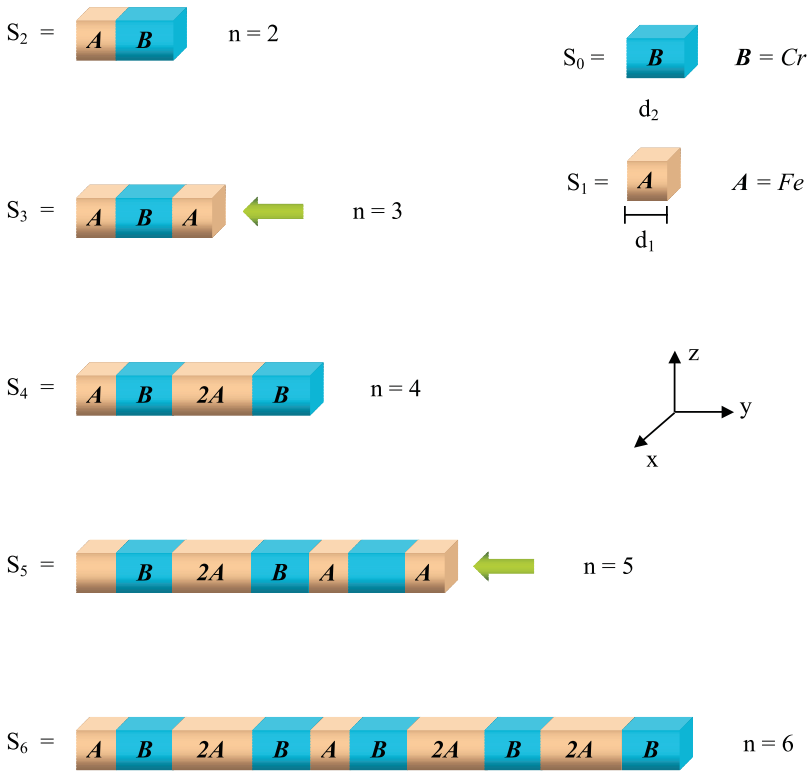

Figure 1. Schematic illustration of the Fibonacci structures considered in this paper.

In recent works [21,22] we have studied the magnetization and magnetoresistance curves of ultra-thin magnetic films (Fe/Cr) grown following the Fibonacci sequence, where, depending on the ratio between the biquadratic and the bilinear exchange coupling terms, a striking self-similar pattern was found. It is the aim of this work to use the magnetization equation of motion technique to study the spin wave spectra in these Fe/Cr(100) quasi-periodic Fibonacci structures, using the experimental magnetic parameters reported by Rezende *et al* [20]. In our specific case we choose Fe as the building block A, with thickness d_1, and Cr as the building block B, with thickness d_2 (see figure 1). Although the bilinear and biquadratic exchange coupling parameters may oscillate as functions of the non-magnetic layer thicknesses (Cr), we can justify the use of their physical parameters in our calculations, since for the quasi-periodic Fibonacci sequence considered here there are only single Cr layers, no matter which generation is considered. Regarding the exchange coupling oscillation as a function of the FM layer thickness, our numerical calculation may be justified for the case where the layers are sufficiently thick.

The plan of this work is as follows: in section 2, we present the method of calculation employed here, which is based on the equation of motion approach, to study the problem of thin magnetic films. The dispersion relation of the spin waves is then determined for the particular trilayer magnetic system, and then generalized for any Fibonacci generation number. Section 3 is devoted to the discussion of the results found in the precedent section, emphasizing their main features. The conclusions are also in section 3.

2. General theory

Before describing our model, let us briefly review the Fibonacci quasi-periodic sequence considered in this work. The Fibonacci structure is of the type called *substitutional sequences*. It is characterized by the nature of its Fourier spectrum, which is dense pure point. Let us first recall the definition of a substitutional sequence. Take a finite set ξ (here $\xi = \mathrm{A}, \mathrm{B}$, A and B being different building blocks) called an *alphabet*, and denote by ξ^* the set of all words of finite length that can be written in this alphabet. Now let ζ be a map from ξ to ξ^* by specifying that ζ acts on a word by substituting each letter (e.g. A) of this word by its corresponding image $\zeta(\mathrm{A})$. A sequence is then called a substitution sequence if it is a fixed point of ζ, i.e. if it remains invariant when each letter in the sequence is replaced by its image under ζ. For the Fibonacci sequence we have the rules $\mathrm{A} \to \zeta(\mathrm{A}) = \mathrm{AB}$, $\mathrm{B} \to \zeta(\mathrm{B}) = \mathrm{A}$.

A quasiperiodic Fibonacci structure can be grown experimentally by juxtaposing the two building blocks A and B in such a way that the nth stage of the structure S_n is given interactively by the rule $S_n = S_{n-1}S_{n-2}$ for $n \geqslant 2$, with $S_0 = \mathrm{B}$ and $S_1 = \mathrm{A}$ (initial conditions). It is also invariant under the transformations $\mathrm{A} \to \mathrm{AB}$ and $\mathrm{B} \to \mathrm{A}$. In our specific case we choose Fe as building block A with thickness d_1 and Cr as building block B with thickness d_2 (see figure 1). The number of building blocks increases according to the Fibonacci number, $F_n = F_{n-1} + F_{n-2}$ (with $F_0 = F_1 = 1$), and the ratio between the number of building blocks A and the number of building blocks B in the sequence is equal to the golden mean number τ. The Fibonacci generations are $S_0 = [\mathrm{B}]$, $S_1 = [\mathrm{A}]$, $S_2 = [\mathrm{AB}]$, $S_3 = [\mathrm{ABA}]$ and so on. Therefore the trilayer Fe/Cr/Fe is the correspondent of the third Fibonacci generation [ABA]. We notice that only *odd* Fibonacci generations have a magnetic counterpart, because they start and finish with Fe (building block A). Observe that for $n > 3$, n being the Fibonacci generation number, the quasiperiodic structure will always be constituted by single Cr layers and single and double Fe ones.

Let us now derive the spin wave dispersion relation using the well known torque equation for the magnetization on film i, i.e.

$$\frac{\mathrm{d}\vec{M}_i}{\mathrm{d}t} = -\gamma \vec{M}_i \times \vec{H}_{\mathrm{eff}} \tag{1}$$

where $\gamma = g\mu_{\mathrm{B}}\hbar$ is the gyromagnetic ratio, g being the Landé factor and μ_{B} the Bohr magneton. $\vec{H}_{\mathrm{eff}}$ is the effective magnetic field acting on $\vec{M}_i$.

For each magnetic film we write a Cartesian coordinate system, called the local axis system, with the z axis coinciding with the equilibrium direction of the magnetization. For each film, the magnetization is then given by

$$\vec{M}_i = M_{iz_i}\hat{e}_{z_i} + m_{iy}\hat{e}_y + m_{ix_i}\hat{e}_{x_i} \tag{2}$$

and we assume that $m_{ix_i}, m_{iy} \ll M_{iz_i}$. Note that the y axis of the local axis systems coincides with the crystalline y axis (we do not need to index the local axis system to the y component). The transformation to connect the components of the magnetization from the original variables is given by (see figure 2)

$$M_{ix} = M_{iz_i}\sin\theta_i + m_{ix_i}\cos\theta_i \qquad M_{iy} = m_{iy} \qquad M_{iz} = M_{iz_i}\cos\theta_i - m_{ix_i}\sin\theta_i. \tag{3}$$

Likewise, the effective magnetic field is expressed as

$$\vec{H}_{\mathrm{eff}} = H_{iz_i}\hat{e}_{z_i} + h_{iy}\hat{e}_y + h_{ix_i}\hat{e}_{x_i}. \tag{4}$$

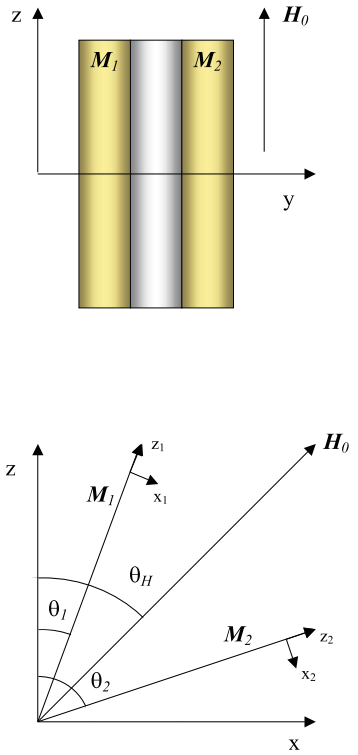

Figure 2. Illustration of the local axis system. The z direction is chosen to stay aligned with the equilibrium position of the magnetization.

Substituting the magnetization (2) and the effective field (4) into (1), and writing only the non-null components, we have

$$\begin{aligned} \frac{\mathrm{d}m_{iy}}{\mathrm{d}t} &= -\gamma_i (M_{iz_i} h_{ix_i} - m_{ix_i} H_{iz_i}) \\ \frac{\mathrm{d}m_{ix_i}}{\mathrm{d}t} &= -\gamma_i (m_{iy} H_{iz_i} - M_{iz_i} h_{iy}). \end{aligned} \tag{5}$$

The relation between the effective field and the total energy is well known, being defined by

$$\vec{H}_{\mathrm{eff}} = -\nabla_M E_{\mathrm{T}}. \tag{6}$$

Here, the total magnetic energy is given by

$$E_{\mathrm{T}} = E_{\mathrm{Z}} + E_{\mathrm{bl}} + E_{\mathrm{bq}} + E_{\mathrm{d}} + E_{\mathrm{ca}} + E_{\mathrm{sa}} \tag{7}$$

where E_{Z}, E_{bl}, E_{bq}, E_{d}, E_{ca} and E_{sa} are respectively the *Zeeman*, *bilinear*, *biquadratic*, *dipolar*, *cubic anisotropy* and *surface anisotropy* energies.

Let us now define all components of the total energy individually. The Zeeman interaction energy is the scalar product of the magnetization by the external applied magnetic field. In the case of N magnetic films, it is given by

$$E_{\mathrm{Z}} = -\sum_{i=1}^{N} d_i \vec{M}_i \cdot \vec{H}_0 \tag{8}$$

where d_i is the width of each FM layer, and $\vec{M}_i$ and $\vec{H}_0$ are the magnetization and the external magnetic field, respectively. The bilinear and the biquadratic energies are defined as

$$E_{\mathrm{bl}} = -\sum_{i=1}^{N-1} J_{\mathrm{bl}} \frac{\vec{M}_i \cdot \vec{M}_{i+1}}{|\vec{M}_i||\vec{M}_{i+1}|} \tag{9}$$

and

$$E_{\mathrm{bq}} = \sum_{i=1}^{N-1} J_{\mathrm{bq}} \left(\frac{\vec{M}_i \cdot \vec{M}_{i+1}}{|\vec{M}_i||\vec{M}_{i+1}|} \right)^2 \tag{10}$$

where J_{bl} and J_{bq} are, respectively, the bilinear and biquadratic exchange constants. The dipolar energy, also called the demagnetizing energy, is given by

$$E_d = 2\pi \sum_{i=1}^{N} d_i (\vec{M}_i \cdot \hat{e}_y)^2. \tag{11}$$

The cubic and surface anisotropy energies can be written in the form

$$E_{\mathrm{ca}} = \sum_{i=1}^{N} \frac{d_i K_{\mathrm{ca}}}{|\vec{M}_i|^4} (M_{ix}^2 M_{iy}^2 + M_{ix}^2 M_{iz}^2 + M_{iy}^2 M_{iz}^2) \tag{12}$$

and

$$E_{\mathrm{sa}} = -\sum_{i=1}^{N} \frac{K_{\mathrm{s}}}{M_i^2} (\vec{M}_i \cdot \hat{e}_y)^2 \tag{13}$$

where K_{s} is the surface anisotropy constant.

To calculate the effective fields h_{ix_i}, h_{iy} and H_{iz_i}, we use

$$h_{ix_i} = -\frac{\partial E_{\mathrm{T}}}{\partial m_{ix_i}} \qquad h_{iy} = -\frac{\partial E_{\mathrm{T}}}{\partial m_{iy}} \qquad \text{and} \qquad H_{iz_i} = -\frac{\partial E_{\mathrm{T}}}{\partial m_{iz_i}}. \tag{14}$$

Writing explicitly the equations of motion for N magnetic films, it is necessary to solve a system of $2N$ equations

$$\begin{aligned} \frac{1}{\gamma_i} \sum_{i=1}^{N} \frac{\mathrm{d}m_{iy}}{\mathrm{d}t} &= M_{iz_i} \left(\frac{\partial E_{\mathrm{T}}}{\partial m_{ix_i}} \right) - m_{ix_i} \left(\frac{\partial E_{\mathrm{T}}}{\partial m_{iz_i}} \right) \\ \frac{1}{\gamma_i} \sum_{i=1}^{N} \frac{\mathrm{d}m_{ix_i}}{\mathrm{d}t} &= m_{iy} \left(\frac{\partial E_{\mathrm{T}}}{\partial m_{iz_i}} \right) - m_{iz_i} \left(\frac{\partial E_{\mathrm{T}}}{\partial m_{iy}} \right) \end{aligned} \tag{15}$$

where N is the total number of layers of type A. In the case of the trilayer Fe/Cr/Fe we have $N = 2$, corresponding to the third Fibonacci sequence ($n = 3$). For the seven-layer case, Fe/Cr/2Fe/Cr/Fe/Cr/Fe, we have $N = 4$, corresponding to the fifth Fibonacci generation ($n = 5$) etc (see figure 1).

Now, using (6), with the help of the total magnetic energy (7), and considering solutions of the type

$$m_{ix_i} = m_{ix_i}^0 \exp(-\mathrm{i}\omega t) \qquad m_{iy} = m_{iy}^0 \exp(-\mathrm{i}\omega t) \tag{16}$$

with $N = 2$ and $i = 1, 2$ we can obtain, after a little algebra,

$$\begin{bmatrix} -\frac{\mathrm{i}\omega}{\gamma} & H_1 & 0 & H_2 \\ -H_3 & -\frac{\mathrm{i}\omega}{\gamma} & H_4 & 0 \\ 0 & H_1 & -\frac{\mathrm{i}\omega}{\gamma} & H_2 \\ H_3 & 0 & -H_4 & -\frac{\mathrm{i}\omega}{\gamma} \end{bmatrix} \begin{bmatrix} m_{1x_1} \\ m_{1y} \\ m_{2x_2} \\ m_{2y} \end{bmatrix} = 0 \tag{17}$$

where

$$H_1 = H_0\cos(\theta_1-\theta_H) + H_{\rm bl}\cos(\theta_1-\theta_2) - \frac{H_{\rm ca}}{2}\,[\sin^2(2\theta_1)-2]$$
$$-2H_{\rm bq}\cos^2(\theta_1-\theta_2) + 4\pi M_{\rm s} - H_{\rm sa} \tag{18}$$
$$H_2 = -H_{\rm bl} + 2H_{\rm bq}\cos(\theta_1-\theta_2) \tag{19}$$
$$H_3 = H_0\cos(\theta_1-\theta_H) + H_{\rm bl}\cos(\theta_1-\theta_2) - 2H_{\rm bq}\cos(\theta_1-\theta_2) - \frac{H_{\rm ca}}{2}\,[4\sin^2(2\theta_1)-2] \tag{20}$$
$$H_4 = -H_{\rm bl}\cos(\theta_1-\theta_2) + 2H_{\rm bq}\cos[2(\theta_1-\theta_2)]. \tag{21}$$

From the resulting 4×4 determinantal condition we find

$$(\omega/\gamma)^4 + \alpha_0(\omega/\gamma)^2 + \alpha_1 = 0 \tag{22}$$

and after some algebraic steps we obtain the dispersion relation for the trilayer case:

$$(\omega/\gamma)^2 = -\alpha_0/2 \pm \sqrt{(\alpha_0/2)^2-\alpha_1} \tag{23}$$

with

$$\alpha_0 = -H_2H_4 + H_1H_4 - H_1H_3 + H_2H_3$$
$$\alpha_1 = -H_1H_4G_1G_4 + H_1H_3G_1G_3 - H_2H_3G_2G_3 + H_2H_4G_2G_4.$$

The coefficients G_i can be obtained from H_i by interchanging $i = 1$ for 2 (layer index).

The four-magnetic-film case can now be treated using the same method as applied for the two-film case. In this way (17) is replaced by ($N = 4$ and $i = 1, 2, 3, 4$)

$$\begin{bmatrix}
-\frac{i\omega}{\gamma} & H_2 & 0 & H_3 & 0 & 0 & 0 & 0\\
-H_5 & -\frac{i\omega}{\gamma} & H_6 & 0 & 0 & 0 & 0 & 0\\
0 & G_1 & -\frac{i\omega}{\gamma} & G_2 & 0 & G_3 & 0 & 0\\
G_4 & 0 & -G_5 & -\frac{i\omega}{\gamma} & G_6 & 0 & 0 & 0\\
0 & 0 & 0 & I_1 & -\frac{i\omega}{\gamma} & I_2 & 0 & I_3\\
0 & 0 & I_4 & 0 & -I_5 & -\frac{i\omega}{\gamma} & I_6 & 0\\
0 & 0 & 0 & 0 & 0 & J_1 & -\frac{i\omega}{\gamma} & J_2\\
0 & 0 & 0 & 0 & J_4 & 0 & -J_5 & -\frac{i\omega}{\gamma}
\end{bmatrix}
\begin{bmatrix} m_{1x_1}\\ m_{1y}\\ m_{2x_2}\\ m_{2y}\\ m_{3x_3}\\ m_{3y}\\ m_{4x_4}\\ m_{4y}\end{bmatrix} = 0. \tag{24}$$

The coefficients H_i, G_i, I_i and J_i can be obtained using the expressions below:

$$X_1 = H_0\cos(\theta_i-\theta_H) + H_{\rm bl}\cos(\theta_i-\theta_{i+1}) - \frac{H_{\rm ca}}{2}\,[\sin^2(2\theta_i)-2]$$
$$-2H_{\rm bq}\cos^2(\theta_i-\theta_{i+1}) + 4\pi M_{\rm s} - H_{\rm sa} \tag{25}$$
$$X_2 = -H_{\rm bl} + 2H_{\rm bq}\cos(\theta_i-\theta_{i+1}) \tag{26}$$
$$X_3 = H_0\cos(\theta_i-\theta_H) + H_{\rm bl}\cos(\theta_i-\theta_{i+1}) - 2H_{\rm bq}\cos[2(\theta_i-\theta_{i+1})] - \frac{H_{\rm ca}}{2}\,[4\sin^2(2\theta_i)-2] \tag{27}$$
$$X_4 = H_{\rm bl}\cos(\theta_i-\theta_{i+1}) - 2H_{\rm bq}\cos[2(\theta_i-\theta_{i+1})] \tag{28}$$
$$Y_1 = H_0\cos(\theta_{i+1}-\theta_H) + H_{\rm bl}[\cos(\theta_i-\theta_{i+1}) + \cos(\theta_{i+1}-\theta_{i+2})] - \frac{H_{\rm ca}}{2}\,[\sin^2(2\theta_{i+1})-2]$$
$$-2H_{\rm bq}[\cos^2(\theta_i-\theta_{i+1}) + \cos^2(\theta_{i+1}-\theta_{i+2})] + 4\pi M_{\rm s} - H_{\rm sa} \tag{29}$$
$$Y_2 = -H_{\rm bl} + 2H_{\rm bq}\cos(\theta_{i+1}-\theta_{i+2}) \tag{30}$$
$$Y_3 = H_0\cos(\theta_{i+1}-\theta_H) + H_{\rm bl}[\cos(\theta_i-\theta_{i+1}) + \cos(\theta_{i+1}-\theta_{i+2})] - 2H_{\rm bq}\{\cos[2(\theta_i-\theta_{i+1})]$$
$$+\cos[2(\theta_{i+1}-\theta_{i+2})]\} - \frac{H_{\rm ca}}{2}\,[4\sin^2(2\theta_{i+1})-2] \tag{31}$$
$$Y_4 = H_{\rm bl}\cos(\theta_{i+1}-\theta_{i+2}) - 2H_{\rm bq}\cos[2(\theta_{i+1}-\theta_{i+2})] \tag{32}$$

in such a way that

$$\left.\begin{array}{llll} X_1 = H_2 & X_2 = H_3 & X_3 = H_5 & X_4 = H_6 \\ Y_1 = G_2 & Y_2 = G_3 & Y_3 = G_5 & Y_4 = G_6 \end{array}\right\} \quad \text{for } i = 1$$
$$Y_1 = I_2 \qquad Y_2 = I_3 \qquad Y_3 = I_5 \qquad Y_4 = I_6 \qquad \text{for } i = 2 \tag{33}$$
$$X_1 = J_2 \qquad X_2 = J_1 \qquad X_3 = J_5 \qquad X_4 = J_4 \qquad \text{for } i = 3$$

with $G_1 = H_3$, $G_3 = I_1$, $G_4 = H_6$ and $G_6 = I_4$.

From the resulting 8×8 determinant condition we obtain the desired dispersion relation, i.e.

$$\left(\frac{\omega}{\gamma}\right)^8 + \alpha_0 \left(\frac{\omega}{\gamma}\right)^6 + \alpha_1 \left(\frac{\omega}{\gamma}\right)^4 + \alpha_2 \left(\frac{\omega}{\gamma}\right)^2 + \alpha_3 = 0 \tag{34}$$

with the α coefficients defined in appendix A.

For the case of nine or more films, we also use the solutions of the type found in (16), with $N = 9$ and $i = 1, 2, \ldots, 9$. Proceeding in a similar way to the two previous cases, we can generalize the spin-wave dispersion relation for any N magnetic films by

$$\left(\frac{\omega}{\gamma}\right)^{2N} + \left[\sum_{j=(2N-2),(2N-4),\ldots}^{2} \sum_{k=0}^{N-2} \alpha_k \left(\frac{\omega}{\gamma}\right)^j \right] + \alpha_{N-1} = 0. \tag{35}$$

3. Numerical results and conclusions

In this section we present numerical results for the spin wave dispersion relation, which can propagate in magnetic thin films following a quasi-periodic Fibonacci sequence. A physical motivation for this is that these structures can exhibit magnetic properties not found in the periodic case. Our results are divided into three groups regarding the physical parameters used in this theoretical calculation, namely the first parameter set, near to the first AF peak (strong bilinear exchange coupling), with $H_{\mathrm{bq}} = -0.1 H_{\mathrm{bl}} = 0.1$ kOe, a second parameter set, near to the first FM–AF transition (moderate bilinear exchange coupling), with $H_{\mathrm{bq}} = -(1/3) H_{\mathrm{bl}} = 0.05$ kOe, and lastly a third set, near to the second AF peak (weak bilinear exchange coupling comparable to the biquadratic exchange coupling), with $H_{\mathrm{bq}} = -H_{\mathrm{bl}} = 0.035$ kOe. For all groups we have the same values for the cubic anisotropy field, $H_{\mathrm{ca}} = 0.5$ kOe, and also for the surface anisotropy field, $H_{\mathrm{sa}} = 2$ kOe.

Figures 3–5 show the spin wave spectra for the seven-layer case, which means four magnetic thin films separated by three non-magnetic spacers. We have considered the three groups of parameters specified above. In all figures we have plotted the frequency shift (in GHz) against the external magnetic field (in kOe). Here dashed curves represent the acoustic modes, while full curves represent the optical mode frequencies. Altogether we have four dispersion curves representing the four magnetic layers. The most pronounced effect of the biquadratic coupling, as observed by comparing the three curves, is to shift the frequency of the optical mode, downwards in the AF and FM phases and upwards in the central region (which corresponds to the 90° magnetic phase). Actually this behaviour has a weak dependence on the magnetic field within each region, but, as far the determination of the critical field is concerned, the values taken at the frontier are excellent approximations to the real ones. Similarly, between the 90° magnetic phases and the saturation the effective anisotropies (cubic and surface) has minimal influence in the spectra.

In a similar way, we have presented in figures 6–8 the spin wave spectra for the much more robust (and sophisticated!) 17-layer case, which means nine magnetic thin films separated by eight non-magnetic spacers. Again we have plotted the frequency shift (in GHz) against the

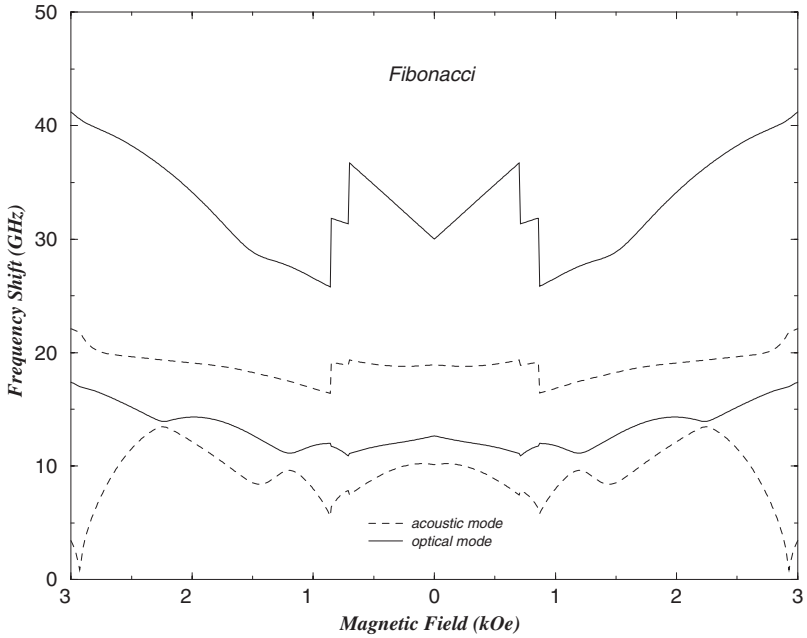

Figure 3. Spin wave dispersion relations for the heptalayer case using the ratio of the biquadratic term and the bilinear one equal to 0.1.

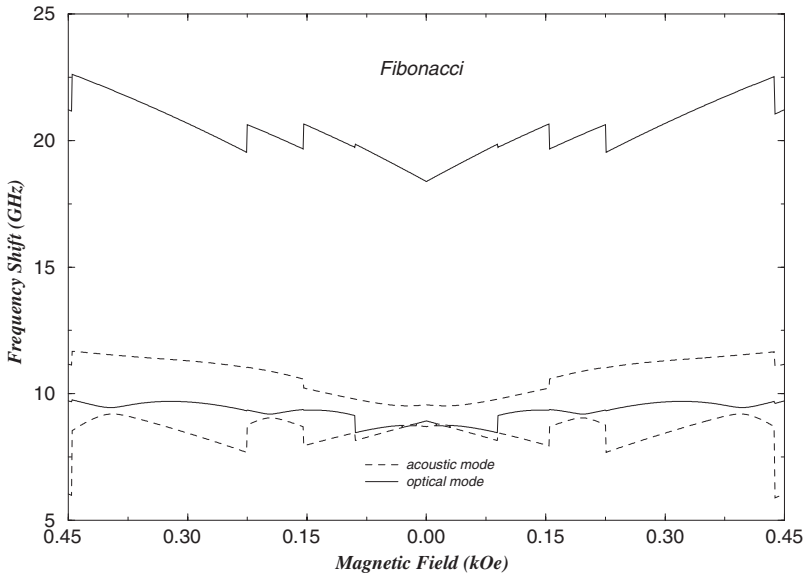

Figure 4. The same as figure 3 but using the ratio between the biquadratic and the bilinear terms equal to one-third.

external magnetic field (in kOe). For the three figures there are now five acoustic modes and four optical modes in the spectra. In figure 6 we can see five curves, where the first one is a partial superimposition between the acoustic mode (dashed curve) and the optical one

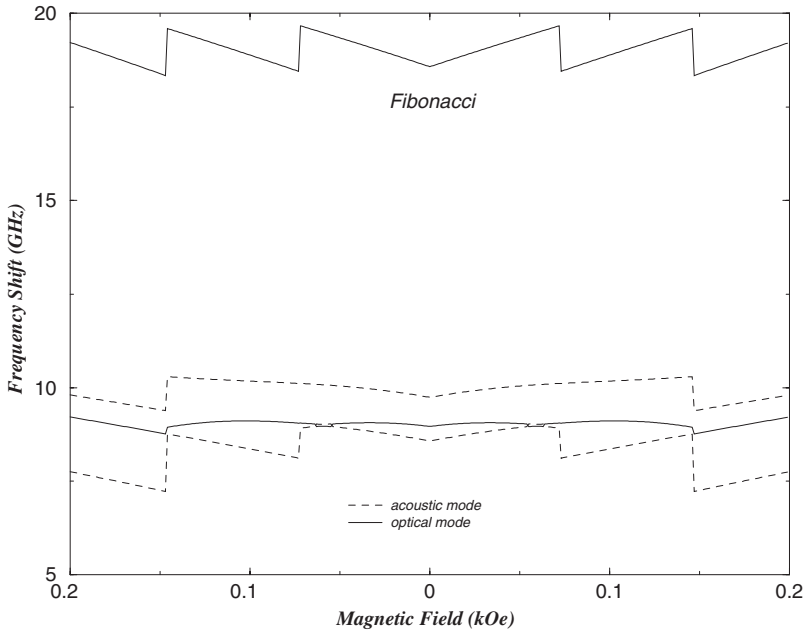

Figure 5. The same as figure 3 but using the ratio equal to unity.

(dotted curve). The second, third and fourth curves are complete superimpositions between the acoustic and optical modes (full curves). The fifth and last curve is a single acoustic mode (dashed curve). In figures 7 and 8 the four first curves represent the total superposition between the acoustic and optical modes (full curves), and the fifth curve represents the optical mode (dashed curve). Reasonable fits to a hypothetical measured magnetization curves can be obtained for AF and FM coupling phases, although it is much more complicated to identify which coupling is the right one. There are some important points that we can infer from this case:

(a) the reduced values of the biquadratic term (figures 6 and 7) are related only to the transition between the 90° magnetic phase and the saturated region, and therefore it is not possible to determine the two coupling fields accurately;
(b) surprisingly, the same behaviour was observed in figure 8 in the region around the second AF peak and
(c) besides these regions, the magnetization curves show qualitatively similar behaviour, although the same restrictions regarding the coupling fields are sustained.

In conclusion we have presented in this work a theory to treat the low-wavenumber spin wave dispersion relation for ultra-thin magnetic films which follow the Fibonacci sequence. In addition to bilinear and biquadratic exchange, our theory takes full account of surface, in-plane uniaxial and cubic anisotropy interactions. We present analytical expressions up to the 17-layer case, and a full expression generalizing any Fibonacci generation number. We have used a three-parameter set, determined by independent fitting, to study the numerical calculations. Furthermore, our theoretical predictions are adequate to extract reliable values for the magnetic parameters involved, since the frequencies of the magnetic excitations depend directly upon the magnetization configuration of each FM layer (see [20] for the Fe/Cr/Fe trilayer case).

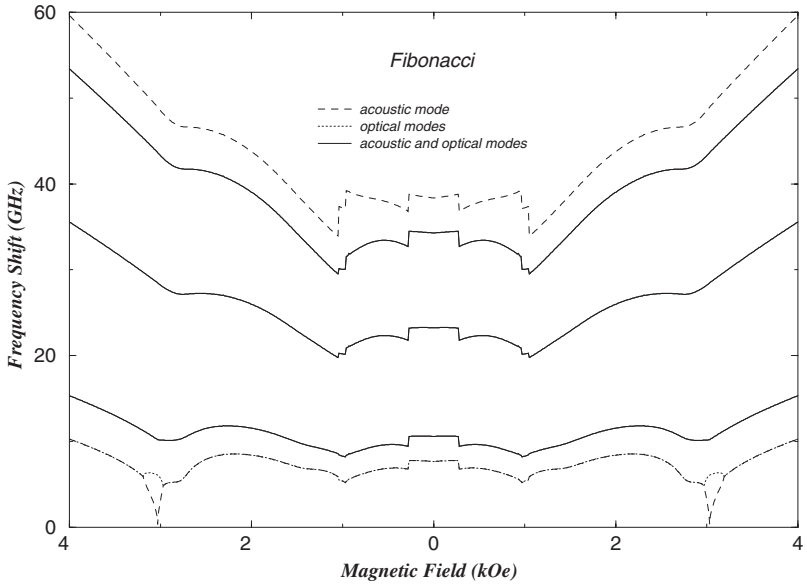

Figure 6. Spin wave dispersion relations for the 17-layer case using the ratio of the biquadratic term and the bilinear one equal to 0.1.

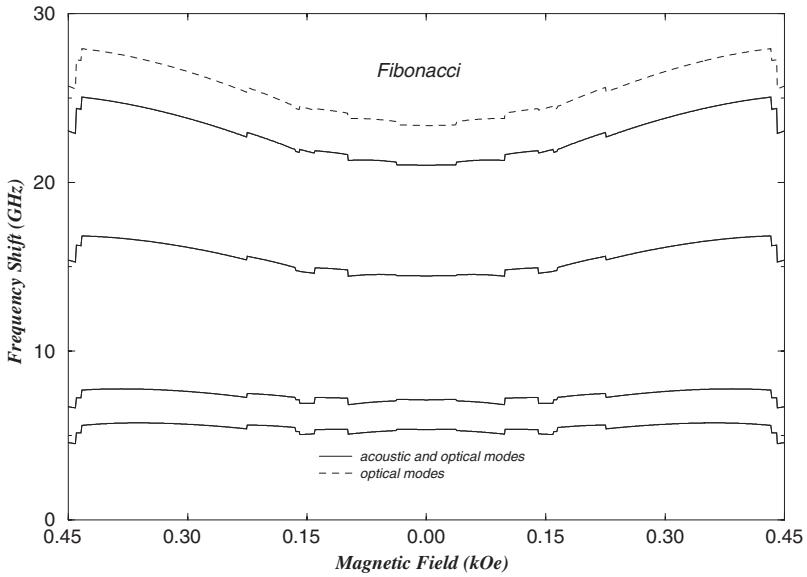

Figure 7. The same as figure 6 but using the ratio between the biquadratic and bilinear terms equal to one-third.

Experimental tools to investigate our theoretical predictions include the magneto-optical Kerr effect (MOKE), Brillouin light scattering (BLS) and ferromagnetic resonance (FMR). Our calculations are adequate for low-wavenumber spin waves, and the analytical expressions derived here can be observed with either BLS experiments (for $q \neq 0$ modes) or FMR techniques (corresponding to the $q = 0$ modes). These techniques are among the best methods

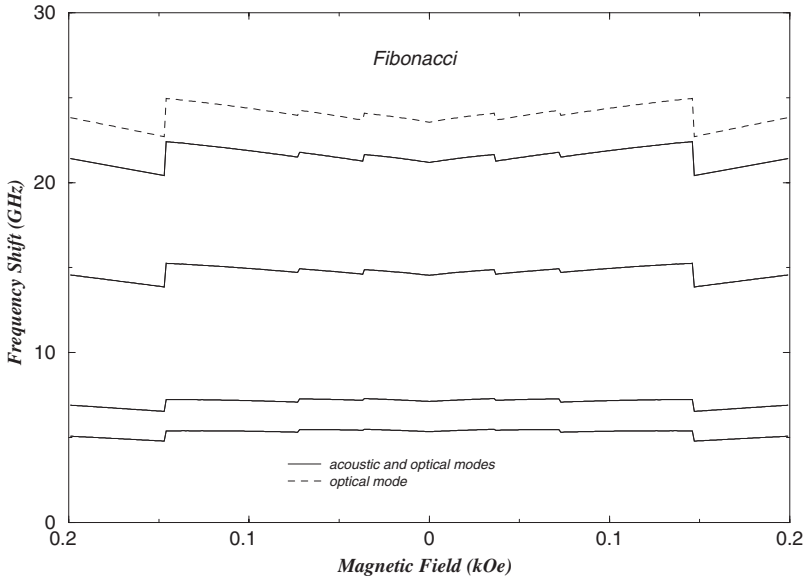

Figure 8. The same as figure 6 but using the ratio equal to unity.

to determine the interlayer exchange coupling between FM films separated by a nonmagnetic metallic spacer, as used in this work, and we hope our results may encourage experimentalists to face them.

Acknowledgments

We thank the Brazilian Research Agencies CAPES-PROCAD and CT-Petro/CNPq for partial financial support.

Appendix A

The α coefficients, used in (34), are given by

$$\alpha_0 = +G_4H_3 + G_1H_6 + I_4G_3 - H_2H_5 - J_2J_5 + J_1I_6 - I_5I_2 + I_1G_6 - G_5G_2 + J_4I_3 \tag{36}$$

$$\begin{aligned}\alpha_1 = {} & +G_1H_6J_4I_3 - I_4G_3J_2J_5 + I_4J_4G_3I_3 + I_4I_1G_6G_3 - G_1H_6J_2J_5 \\ & +G_1H_6I_1G_6 + G_1H_6J_1I_6 - G_1H_6I_5I_2 - I_1G_6J_2J_5 + I_1G_6J_1I_6 \\ & +H_5H_2I_5I_2 - H_5H_2J_4I_3 + G_4H_3J_1I_6 + I_5I_2J_2J_5 - I_5J_1I_3J_5 \\ & -J_4I_2I_6J_2 + J_4J_1I_3I_6 - G_4H_3J_2J_5 + G_4G_1H_6H_3 - G_4H_2H_6G_2 \\ & -H_5G_1G_5H_3 + H_5H_2G_5G_2 + H_5H_2J_2J_5 - H_5H_2I_4G_3 - H_5H_2I_1G_6 \\ & -H_5H_2J_1I_6 - I_4G_2G_6I_2 - G_5I_1I_5G_3 - G_5G_2J_4I_3 - G_5G_2J_1I_6 \\ & +G_5G_2I_5I_2 + G_5G_2J_2J_5 + G_4I_4H_3G_3 + G_4H_3J_4I_3 - G_4H_3I_5I_2\end{aligned} \tag{37}$$

$$\begin{aligned}\alpha_2 = {} & -G_1H_6J_4I_2I_6J_2 + G_1H_6J_4J_1I_3I_6 - G_1H_6I_5J_1I_3J_5 - G_1H_6T\,I_1G_6J_2J_5 \\ & +G_1H_6I_1G_6J_1I_6 + G_1H_6I_5I_2J_2J_5 - H_5H_2J_4J_1I_3I_6 + H_5H_2I_1G_6J_2J_5 \\ & +G_4G_1H_6H_3J_4I_3 + G_4H_2H_6G_2J_2J_5 + G_4G_1H_6H_3J_1I_6 - G_4G_1H_6H_3J_2J_5 \\ & -G_4H_2H_6I_1I_5G_3 - G_4H_2H_6G_2J_4I_3 + G_4H_2H_6G_2I_5I_2 - G_4H_2H_6G_2J_1I_6\end{aligned}$$

$$
\begin{aligned}
&-H_5G_1G_5H_3J_4I_3 - H_5G_1I_4H_3G_6I_2 + H_5G_1G_5H_3I_5I_2 - H_5G_1G_5H_3J_1I_6\\
&+H_5G_1G_5H_3J_2J_5 - H_5H_2I_1G_6J_1I_6 + H_5H_2J_4I_2I_6J_2 + H_5H_2I_5J_1I_3J_5\\
&-H_5H_2I_5I_2J_2J_5 - G_5G_2I_5I_2J_2J_5 + G_5G_2I_5J_1I_3J_5 + G_5G_2J_4I_2I_6J_2\\
&-G_5I_1J_4G_3I_6J_2 + I_4G_2G_6I_2J_2J_5 - I_4G_2G_6J_1I_3J_5 - I_4I_1G_6G_3J_2J_5\\
&-H_5H_2I_4J_4G_3I_3 - H_5H_2I_4I_1G_6G_3 + H_5H_2G_5I_1I_5G_3 + H_5H_2I_4G_3J_2J_5\\
&+H_5H_2I_4G_2G_6I_2 - H_5H_2G_5G_2J_2J_5 + H_5H_2G_5G_2J_4I_3 - H_5H_2G_5G_2I_5I_2\\
&+H_5H_2G_5G_2J_1I_6 - G_4H_3I_5J_1I_3J_5 + G_4I_4H_3J_4G_3I_3 - G_4I_4H_3G_3J_2J_5\\
&+G_4H_3J_4J_1I_3I_6 - G_5H_3J_4I_2I_6J_2 - G_4G_1H_6H_3I_5I_2 + G_4H_3I_5I_2J_2J_5 \qquad (38)
\end{aligned}
$$

$$
\begin{aligned}
\alpha_3 = {}&+H_5H_2G_5G_2I_5I_2J_2J_5 - H_5H_2G_5G_2I_5J_1I_3J_5 - H_5H_2G_5G_2J_4I_2I_6J_2\\
&+H_5H_2G_5G_2J_4J_1I_3I_6 - H_5H_2G_5I_1I_5G_3J_2J_5 + H_5H_2G_5I_1J_4G_3I_6J_2\\
&-H_5H_2I_4G_2G_6I_2J_2J_5 + H_5H_2I_4G_2G_6J_1I_3J_5 + H_5H_2I_4G_2G_6J_1I_3J_5\\
&+H_5H_2I_4I_1G_6G_3J_2J_5 - H_5G_1G_5H_3I_5I_2J_2J_5 + H_5G_1G_5H_3I_5J_1I_3J_5\\
&+H_5G_1G_5H_3J_4I_2I_6J_2 - H_5G_1G_5H_3J_4J_1I_3I_6 + H_5G_1I_4H_3G_6I_2J_2J_5\\
&-H_5G_1I_4H_3G_6J_1I_3J_5 - G_4H_2H_6G_2I_5I_2J_2J_5 + G_4H_2H_6G_2I_5J_1I_3J_5\\
&+G_4H_2H_6G_2J_4I_2I_6J_2 - G_4H_2H_6G_2J_4J_1I_3I_6 + G_4H_2H_6I_1I_5G_3J_2J_5\\
&-G_4H_2H_6I_1J_4G_3I_6J_2 + G_4G_1H_6H_3I_5I_2J_2J_5 - G_4G_1H_6H_3I_5J_1I_3J_5\\
&-G_4G_1H_6H_3J_4I_2I_6J_2 + G_4G_1H_6H_3J_4J_1I_3I_6. \qquad (39)
\end{aligned}
$$

References

[1] Shechtman D, Blech I, Gratias D and Cahn J W 1984 *Phys. Rev. Lett.* **53** 1951
[2] Levine D and Steinhardt P J 1984 *Phys. Rev. Lett.* **53** 2477
[3] Steinhardt P J and Ostlund S (ed) 1987 *The Physics of Quasicrystals* (Singapore: World Scientific)
[4] Jarić M V (ed) 1988 *Introduction to Quasicrystals* (New York: Academic)
[5] Chaikin P M and Lubenlky T C 1995 *Principles of Condensed Matter Physics* (Cambridge: Cambridge University Press)
[6] Penrose R 1974 *Bull. Inst. Math. Appl.* **10** 266
[7] Merlin R, Bajema K, Clarke R, Juang F-Y and Bhattacharya P K 1985 *Phys. Rev. Lett.* **55** 1768
[8] Roy C L and Kan A 1995 *Phys. Rev.* B **49** 14 949
[9] Kolár M, Ali M K and Nori F 1991 *Phys. Rev.* B **43** 1034
[10] Vasconcelos M S and Albuquerque E L 1998 *Phys. Rev.* B **57** 2826
[11] Kohmoto M, Kadanoff L P and Tang C 1983 *Phys. Rev. Lett.* **50** 1870
Kohmoto M and Banavar J R 1986 *Phys. Rev.* B **34** 563
Kohmoto M, Sutherland B and Iguchi K 1987 *Phys. Rev. Lett.* **58** 2436
Kohmoto M, Sutherland B and Tang C 1987 *Phys. Rev.* B **35** 1020
[12] Luck J M and Petritis D 1986 *J. Stat. Phys.* **42** 289
[13] Petri A and Ruocco G 1995 *Phys. Rev.* B **51** 11 399
[14] See articles Bland J A C and Heinrich B (ed) 1994 *Ultrathin Magnetic Structures* vols 1 and 2 (Berlin: Springer)
[15] Grünberg P, Schreiber R, Pang Y, Brodsky M O and Sowers H 1986 *Phys. Rev. Lett.* **57** 2442
[16] Baibich M N, Broto J M, Fert A, Nguyen Van Dau F, Petroff F, Etienne P, Creuzet G, Friederich A and Chazelas J 1988 *Phys. Rev. Lett.* **61** 2477
[17] Parkin S S P, More N and Roche K P 1990 *Phys. Rev. Lett.* **64** 2304
[18] Ruhrig M, Shafer R, Hubert A, Mosler R, Wolf J A, Demokritov S and Grünberg P 1991 *Phys. Status Solidi* a **125** 635
[19] Hillebrands B 1990 *Phys. Rev.* B **41** 530
[20] Rezende S M, Chesman C, Lucena M A, Azevedo A, Aguiar F M and Parkin S S P 1998 *J. Appl. Phys.* **84** 958
[21] Bezerra C G, de Araujo J M, Chesman C and Albuquerque E L 1999 *Phys. Rev.* B **60** 9264
[22] Bezerra C G, de Araujo J M, Chesman C and Albuquerque E L 2001 *J. Appl. Phys.* **89** 2862